Diffusion of α-Chymotrypsin in Solution-Crowded Media. A Fluorescence Recovery after Photobleaching Study

Isabel Pastor,*,† Eudald Vilaseca,† Sergio Madurga,† Josep Lluís Garcés,‡ Marta Cascante,§ and Francesc Mas†

Department of Physical Chemistry and Research Institute of Theoretical and Computational Chemistry (IQTCUB) of University of Barcelona, C/ Martí i Franquès, 1. E-08028 Barcelona, Spain, Department of Chemistry, University of Lleida (UdL), Lleida, Spain, and Department of Biochemistry and Molecular Biology and Institute of Biomedicine (IBUB) of University of Barcelona and IDIBAPS, Barcelona, Spain

Received: November 13, 2009; Revised Manuscript Received: January 28, 2010

Fluorescence recovery after photobleaching (FRAP) is one of the most powerful and used techniques to study diffusion processes of macromolecules in membranes or in bulk. Here, we study the diffusion of α-chymotrypsin in different crowded (Dextran) in vitro solutions using a confocal laser scanning microscope. In the considered experimental conditions, confocal FRAP images could be analyzed applying the uniform circular disk approximation described for a nonscanning microscope generalized to take into account anomalous diffusion. Considering the slow diffusion of macromolecules in crowded media, we compare the fitting of confocal FRAP curves analyzed with the equations provided by the Gaussian and the uniform circular disk profile models for nonscanning microscopes. As the fitted parameter variation with the size and concentration of crowders is qualitatively similar for both models, the use of the uniform circular disk or the Gaussian model is justified for these experiments. Moreover, in our experimental conditions, α-chymotrypsin shows anomalous diffusion ($\alpha < 1$), depending on the size and concentration of Dextran molecules, until a high concentration and high size of crowding agent are achieved. This result indicates a range of validity of the idealized fitting expressions used, beyond which other physical phenomena must be considered.

Introduction

Studies of diffusion-controlled reaction of biological macromolecules are usually performed in dilute solutions (in vitro). However, the high concentration of macromolecules in intracellular environments (in vivo) results into nonspecific interactions (macromolecular crowding), which have a great influence on the kinetics and thermodynamics of possible reactions that occur in these systems.[1–8] Specifically, the living cells have many compartments with different geometries. Regarding the cell membrane, we may consider it as a two-dimensional (2D) highly organized medium mainly containing proteins and lipids. Both substances may undergo translational and rotational diffusion processes, but their mobility strongly depends on their size and the environment properties. In the literature there are Monte Carlo (MC) simulation studies of diffusion in 2D media[9–16] showing that the lateral diffusion is anomalous for short times and normal for long times. This fact implies that the diffusion coefficients depend on time and this dependency is described by scale laws, whose exponents depend, in turn, on the size and mobility of the crowding molecules.[10–17] Such simulations have also been performed in 3D,[17–19] leading to results that are in satisfactory agreement with experimental data, showing, for example, that the protein diffusion in cell cytoplasm is reduced considerably.[20–23]

To date, many experimental techniques have been used to study biophysical properties of protein and macromolecules in dilute solutions.[24] Nevertheless, few of them are able to study the properties of a protein in a solution with a high concentration of other macromolecules. Among these techniques, those using fluorescent molecules, like fluorescence correlation spectroscopy (FCS)[20–23,25–31] and fluorescence recovery after photobleaching (FPR or FRAP),[9,32–41] stand out. In this study we have used FRAP because of its special usefulness for studying molecular dynamics, mainly diffusion processes.

As these experimental techniques need a theoretical background to interpret the obtained results, there is an important effort to perform theoretical analysis of this kind of experiments in 2D[32,34,37,39,48] and 3D.[38,41] Most of the proposed theoretical procedures are based on the one presented by Axelrod et al. in 1976.[42] In that work, they studied several idealized cases and distinguished the diffusion monitored by a laser beam having a Gaussian intensity profile from the diffusion monitored by a laser beam having a uniform circular disk profile. Axelrod and co-workers also stated that when the bleaching is performed with a stationary laser beam that is either Gaussian or uniform, the resulting "laser beam intensity profile is intermediate between Gaussian and uniform disc".[41,42]

Nowadays the majority of photobleaching experiments are performed with confocal laser scanning microscopes (confocal FRAP). An important number of manuscripts explain how, from Axelrod et al. equation[42] (Gaussian profile approximation) for stationary lasers, it is possible to study the diffusion of tracer particles (e.g., proteins) in 2D or 3D media when a confocal FRAP is employed.[38–41,43–46,48] But, normally in 2D media confocal FRAP experimental curves can be examined using Soumpasis equation[47] (uniform circular disk profile approxima-

* To whom correspondence should be addressed. E-mail: i.pastor@ub.edu. Fax: (+34) 934021231. Phone: (+34) 934020138.

† Department of Physical Chemistry and Research Institute of Theoretical and Computational Chemistry, University of Barcelona.

‡ University of Lleida.

§ Department of Biochemistry and Molecular Biology and Institute of Biomedicine, University of Barcelona.

10.1021/jp910811j
Published on Web 03/03/2010

TABLE 1: Characteristics of Dextrans Used As Crowding Agent: M_p, M_n, M_w are the Peak Value, Number Average, and Weight Average of Molecular Mass, M_w/M_n is the Polydispersity Index, and R_g Is the Radius of Gyration

Dextran	M_p (kDa)	M_n (kDa)	M_w (kDa)	M_n/M_w	R_g (nm)
D1	4.4	3.3	5.2	1.60	1.7
D2	43.5	35.6	48.6	1.37	5.8
D3	276.5	236.3	409.8	1.73	17

tion) for nonscanning microscope.[48] This approximation is valid for the more usual experimental conditions, because in these cases the postbleach profile does not depend on how the photobleaching was performed but on the shape of the initial postbleached region. However, a scanning confocal bleaching laser profile can be approximated by a Gaussian function for small bleached regions of interest (ROIs), no greater than 3 μm of radius, and high percentages of bleaching, greater than 50%.[41,48] In fact, a recent study of Kang et al.[48] shows that in some experimental conditions the Axelrod et al. method for Gaussian profile can be used to analyze the recovery curves. Moreover, in our experiments on diffusion in crowded media, where the diffusion of tracer molecules is slower than in dilute solution, the diffusion during the bleaching can be considered negligible as in FRAP experiments performed with a stationary laser.[42,45] For these reasons, we think that it would be very useful to compare the results obtained with the Soumpasis equation[47] and with the Axelrod et al. equation[42] in the analysis of confocal FRAP curve obtained in a given experimental conditions.

In this work, we study the diffusion of a model protein (α-chymotrypsin, pI = 5.4) using FRAP in highly confined media in vitro with two objectives; on the one hand, to study experimentally the temporal dependence of its diffusion coefficient, and on the other hand, to compare the results obtained when the Gaussian profile or the uniform circular disk profile approximations are used in the interpretation of the experimental curves. The α-chymotrypsin protein was selected for this study due to the absence of known interactions with Dextrans, the macromolecules chosen as obstacles (crowding agents) and because its size (R_H = 2.33 nm) is intermediate between those of the selected crowding agents. Moreover, its isoelectric point is 5.4, meaning that, under the used 7.4 pH buffer, our protein is negatively charged. The use of a charged protein reduces the risk of aggregation, which is higher in crowded media.

Materials and Methods

Chemicals. Alpha-chymotrypsin (E.C. 3.4.21.1) from bovine pancreas type II (60 Umg^{-1}), which was used without further purification, fluorescein isothiocyanate, and glycerol were purchased from Sigma-Aldrich Chemical (Milwaukee, WI). Dextrans with different molecular weights were all purchased from Fluka (Buchs, Switzerland). The molecular weights (M_p, M_n, and M_w) and rate polydispersity indexes (M_n/M_w) of the used Dextrans are listed in Table 1 where further details on their approximate radii of gyration (R_g) are also included. The molecular weight values are those reported by the supplier, while R_g values were estimated from molecular weight data using experimental relationships from literature.[49,50] All other chemicals were of analytical or spectroscopic reagent grade. Sodium phosphate buffers (10 mM, pH = 7.4 and 0.2 M, pH = 8) were prepared with deionized doubly distilled water.

Labeling of α-chymotrypsin. α-chymotrypsin has a molecular weight around 23 000 Da, whereas the molecular weight of fluorescein isothiocyanate (FITC) is ~ 389.4 Da, which is rather low in comparison to the protein. Nonspecific covalent amino terminal labeling of α-chymotrypsin with FITC was performed by adding the fluorophore to a protein solution in a 10:1 molar ratio in 0.2 M phosphate buffer at pH 8.0. The labeling reaction was carried out for 30 min at room temperature and the unreacted dye was removed with exhaustive dialysis during 48 h. The dye/protein ratio after labeling was 0.6, an estimation obtained from absorbance measurements at 490 and 280 nm, respectively. The molar absorption coefficient of bound fluorescein at the wavelength of 490 nm was 72 800 M^{-1} cm^{-1}.[51]

Fluorescence Recovery after Photobleaching. A Leica TCS SP2 UV scanning confocal microscope equipped with a FRAP software package was used to conduct the FRAP experiments and display and export the FRAP data. FRAP experiments were carried out with a ×63, 1.25 NA water-immersion objective, using a 488 nm Ar^+ laser line at 25 °C and a 8% of relative intensity. Fluorescence emission was collected using the 500−530 nm band-pass filter. Photobleaching illumination was performed using a 476, 488, 496, and 514 nm Ar^+ laser line at 25 °C and a 100% of relative intensity to bleach a circular ROI with a diameter of 4.1 μm. All images were acquired at 512 × 512 pixel resolution and using a 22.5 μm pinhole. The total ROI intensity was collected as a function of time at increments of 0.28 ms during 70 s, and measurements were repeated 6 times for each sample. Our samples were composed of a low concentration (8.55 × 10^{-6} M) of the FITC-protein complex diffusing in an aqueous buffer (phosphate buffered pH = 7.4) in which crowding agents were dissolved at a concentration up to 350 mg/mL. Samples of 30 μL were placed in a spherical cavity microscope slide and were equilibrated for 15 min on a temperature-regulated microscope stage at 25 °C. In these experimental conditions, the contribution to the recovery from diffusion along axial direction is negligible,[43] thus the diffusional medium was considered as 2D. This assumption is fulfilled when the bleached area forms a near cylindrical shape through the sample, as it occurs in a circular bleach spot of a reasonable diameter.[46]

Anomalous Diffusion. A diffusion process taken by a solute in dilute solution is described with the well-known Einstein−Smoluchowski ®equation

$$\langle r^2(t)\rangle = (2d)Dt \tag{1}$$

where d is the topological dimension of the medium where the process is embedded and D is the solute diffusion coefficient. In crowded media, typically in vivo and in a great number of in vitro processes, the existence of different macromolecular species, proteins, nucleic acids, organelles, etc., hinders the diffusion process. In these cases, eq 1 must be generalized for situations of anomalous diffusion[52–58] as

$$\langle r^2(t)\rangle = (2d)\Gamma t^{\alpha} \tag{2}$$

where α is defined as the anomalous exponent ($0 < \alpha < 1$ is the case of subdiffusion and $\alpha > 1$ holds for the case of superdiffusion) and Γ is a generalized transport coefficient, also known as anomalous diffusion coefficient, of units [length^2/time$^\alpha$], defined as

$$\Gamma = \frac{\omega^2}{(2d)\tau_D^{\alpha}} \tag{3}$$

where τ_D is a characteristic residence time of the solute molecule in a volume of a characteristic length ω (beam area). This definition allows introducing a generalized time-dependent diffusion coefficient function, $D(t)$ as

$$D(t) \equiv \frac{\langle r^2(t)\rangle}{(2d)t} = \frac{1}{(2d)}\frac{\omega^2}{\tau_D^2}t^{\alpha-1} = D^{\text{eff}}\left(\frac{t}{\tau_D}\right)^{\alpha-1} \quad (4)$$

which can be put in terms of an apparent/effective diffusion coefficient, D^{eff} defined as[23]

$$D^{\text{eff}} \equiv D(\tau_D) = \frac{1}{(2d)}\frac{\omega^2}{\tau_D} \quad (5)$$

In fractal media, where there is no characteristic length scale, true anomalous diffusion processes are expected at all scales, and the anomalous diffusion exponent can be related with the fractal dimension of the random walk trajectory, d_w, as $\alpha = 1/d_w$.[54] But, many anomalous diffusion processes in crowded media have a characteristic length scale determined by various parameters such as the size of the solutes and the size and concentration of the obstacles of the medium.[23] The analysis of the trajectory of a particle diffusing in such systems shows that for mean-square displacements smaller than this characteristic length, the diffusion is normal, corresponding to a diffusion process in a solution without obstacles. Similarly, for mean-square displacements greater than the characteristic length, a normal diffusion is also observed, corresponding now to a diffusion process in a dense medium with a lower, but constant, diffusion coefficient. For the intermediate mean-square displacements, diffusion is found to be anomalous.[55] For this intermediate regime there is a crossover time from anomalous diffusion at short times to normal diffusion at long times.[56] Monte Carlo simulations of diffusion processes in presence of obstacles corroborate this effect and give a crossover time between the two behaviors.[10,57] This crossover time can be obtained from log $D(t)$ (given by eq 4) versus log(t) curves, which start at the value of the diffusion coefficient in a solution without obstacles, and decrease linearly with a slope related to the anomalous diffusion exponent, α, until they reach to a limiting normal diffusion coefficient corresponding to the crowded media, D^*. The intersection between the slope of the linear decreasing (anomalous diffusion regime) and the line corresponding to the final and constant value of the diffusion coefficient (normal diffusion in a dense medium) yields the crossover time between these two behaviors.[56]

Theoretical Interpretation of FRAP Curves. The main results from FRAP experiments are the curves representing the mean fluorescence intensity recovery in the bleached circular ROI with time. The fluorescence intensity at each time is more conveniently represented in terms of the fractional fluorescence, $f_K(t)$, defined by

$$f_K(t) = \frac{F_K(t) - F_K(0)}{F_K(\infty) - F_K(0)} \quad (6)$$

where $F_K(0)$ is the initial fluorescence after bleaching, $F_K(t)$ is the observed fluorescence at time $t \geq 0$ and $F_K(\infty)$ is the final fluorescence at infinite time. These terms are K-dependent, where K expresses the amount of bleaching induced at time t.

Although a confocal laser scanning microscope was used, the uniform circular disk profile approximation,[38,43,44,46,48] described first in 1983 by Soumpasis,[47] is a suitable model to study our confocal FRAP curves. In fact, according to Pucadyil and Chattopadhyay work of 2006,[38] the fluorescence recovery curve can be analyzed using the following equation

$$F(t) = [F_\infty - F_0][\exp(-2\tau_D/t)(I_0(-2\tau_D/t) + I_1(-2\tau_D/t))] + F_0 \quad (7)$$

where $F(t)$ is the normalized mean fluorescence intensity in the bleached ROI at time t; F_∞ is the recovered fluorescence at time $t = \infty$; F_0 is the bleached fluorescence intensity at time $t = 0$; and I_0 and I_1 are the modified Bessel Functions.

On the other hand, as described by Kang et al.,[48] under our experimental conditions the initial postbleach profile is well described as a Gaussian function. For this reason, we think that our curves can be studied with the classical Gaussian intensity prolife approximation described first by Axelrod et al.[42] in 1976, where the fluorescence recovery is given by

$$F(t) = \sum_{n=1}^{\infty} = \frac{(-k)^n}{n!}\frac{1}{1 + (n(1 + 2t/\tau_D))} \quad (8)$$

where $F(t)$ is the normalized mean fluorescence intensity at a time t in the bleached ROI, the parameter κ is related to the bleach depth, and τ_D is the characteristic time, defined in terms of the transport generalized coefficient Γ and the beam area, ω.

In case the particle's motion is constrained to anomalous diffusion, it is possible to modify eq 8 to include the diffusion time-dependence, like Webb group describes in detail.[32,34] In this case fluorescence recovery is given by

$$F(t) = \left\{F_0\sum_{n=1}^{\infty}\frac{(-\kappa)^n}{n!}\frac{1}{1 + (n(1 + 2(t/\tau_D)^\alpha)}\right\}R + (1 + R)F_0 \quad (9)$$

where F_0 is the fluorescence intensity immediately after bleaching; R is the mobile fraction, defined as $R = (F_\infty - F_0)/(F^0 - F_0)$, where F^0 is the intensity before bleaching and F_∞ is the fluorescence intensity as $t \rightarrow \infty$; and α is the anomalous coefficient, which is related to Γ and ω through $\tau_D = (\omega^2/\Gamma)^{1/\alpha}$ (see eq 3). Recently, a mathematical method using fractional dynamics[46] has been applied to derive eq 9 in some particular cases of subdiffusion.[40]

The series expression in eq 8 can be approximate for low values of percent of bleach[58] by

$$F(t) = \frac{F_0 + F_\infty(t/t_{1/2})}{1 + (t/t_{1/2})} \quad (10)$$

where $t_{1/2}$ is the half time for recovery, which is related with τ_D by $t_{1/2} = \beta\tau_D$. β is an empirical parameter ($1 < \beta < 2$) that depends on the bleach depth. Following this approximation, Feder et al.[32] simplified eq 8 by

$$F(t) = \frac{F_0 + F_\infty(t/t_{1/2})^\alpha}{1 + (t/t_{1/2})^\alpha} \quad (11)$$

and validated it for bleach depths up to 70%. Equations 10 and 11 are used on some occasions[32,34,35] instead of expressions 8 and 9, for normal anomalous diffusion respectively, to analyze FRAP curves.

If anomalous diffusion takes place, eq 7 can be modified to include the diffusion time-dependence for a uniform circular

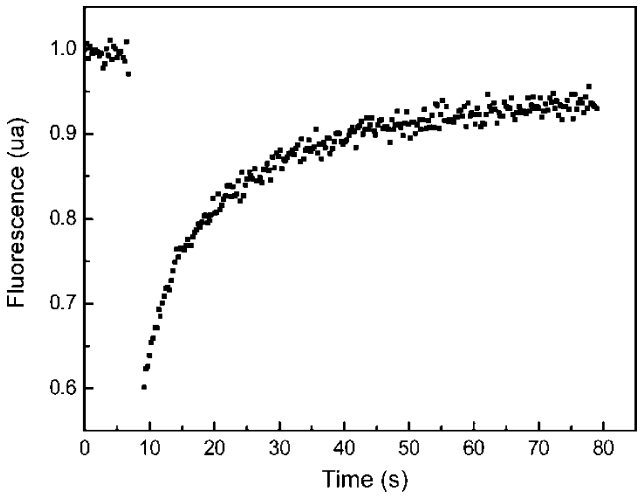

Figure 1. FRAP curve obtained for the solution of α-chymotrypsin in 88% glycerol−water mixture

disk profile, following a similar methodology used by Webb group[32,34] for Gaussian profile. In this case FRAP response becomes

$$F(t) = [F_\infty - F_0][\exp(-2(\tau_D/t)^\alpha)(I_0(-2(\tau_D/t)^\alpha) + I_1(-2(\tau_D/t)^\alpha)] + F_0 \quad (12)$$

where α is the anomalous coefficient.

As we have performed our experiments with a scanning confocal microscope, it is clear that our experimental data should be treated with the uniform circular disk model. However, as we have a small ROI with high percentages of bleaching and the diffusion during photobleaching is probably negligible because of the highly concentrated and/or viscous medium, we have decided to consider both models, uniform circular disk and Gaussian profile. The comparison of both procedures has enabled us to establish interesting correlations among them. In both cases MATLAB (The Mathworks, Natck, MA) was used to develop the routine to fit experimental data and extract the time constant, τ_D, and the anomalous coefficient, α. The goodness of the fitting was judged in terms of χ^2 value and weighted residuals.

Results and Discussion

Our work has a double objective. On the one hand, we want to determine whether the two FRAP expressions described before (eqs 9 and 12) allow us to find the same type of answer in our experiments. On the other hand, we want to investigate if there is an anomalous diffusion phenomenon due to crowding instead of an increase of viscosity in the experimental system we have considered.

With these purposes, we have studied in a first step the diffusion of α-chymotrypsin in a highly viscous medium such as an 88% glycerol−water mixture (μ = 147.494 mPa s).[60] Figure 1 shows the FRAP curve obtained in our experiments. We could use successfully both analysis models to fit these experimental data, and in both cases indeed the fitting with eqs 9 and 12 yielded $\alpha = 1.0 \pm 0.1$. In Table 2 the parameter values for the diffusion of α-chymotrypsin in 88% glycerol−water mixture obtained using both fitting models are shown. It can also be seen that the obtained values for τ_D are quite similar for both models. From these data, we can conclude that the diffusion of α-chymotrypsin in viscous media is slower than in a dilute solution (Buffer) but it continues being normal diffusion. On the other hand, although the data collected with the two expressions are very similar, we need to compare more results to conclude whether the two considered fitting models are equivalent to analyze our FRAP experimental curves. We have also calculated the effective diffusion coefficient (D^{eff}) using eq 5. Both models yield a quite similar result ($\sim 7.3 \pm 0.6$ μm^2 s^{-1}) which is slightly higher than that obtained from Stokes−Einstein equation for the diffusion of a spherical particle in a homogeneous medium with a viscosity similar to the 88% glycerol−water mixture ($D^{eff} = 7.0 \pm 0.1$ μm^2 s^{-1}). This theoretical estimate is in good agreement with the experimentally found values.

TABLE 2: Experimental Parameters Associated with the Diffusion Process of α-Chymotrypsin in 88% Glycerol−water Mixture

fitting model	τ_D (s)	α	D^{eff} (μm^2 s^{-1})
Gaussian	7.8 ± 0.5	1.0 ± 0.1	7.3 ± 0.5
uniform	7.7 ± 0.6	1.0 ± 0.1	7.2 ± 0.6

TABLE 3: Experimental Parameters Associated with the Diffusion Process of α-Chymotrypsin As a Function of Size and Concentration of Crowding Agents Assuming a Gaussian Profile Model

crowder	C (mg/mL)	τ_D (s)	α	D^{eff} (μm^2/s)
D1	100	0.6 ± 0.1	1.0 ± 0.1	101.6 ± 10.8
	200	2.1 ± 0.1	0.8 ± 0.1	26.7 ± 1.6
	300	5.5 ± 0.3	0.8 ± 0.1	10.4 ± 0.6
D2	50	7.4 ± 0.3	0.9 ± 0.1	7.7 ± 0.3
	100	7.5 ± 0.4	0.8 ± 0.1	7.6 ± 0.4
	200	8.4 ± 0.3	0.8 ± 0.1	6.8 ± 0.2
	300	14.7 ± 0.2	0.7 ± 0.1	3.9 ± 0.1
D3	50	7.2 ± 0.3	0.8 ± 0.1	7.9 ± 0.4
	100	10.5 ± 0.3	0.7 ± 0.1	5.3 ± 0.1
	200	10.8 ± 1.0	0.7 ± 0.1	5.3 ± 0.5
	300	32.6 ± 1.0	0.9 ± 0.1	1.7 ± 0.1

TABLE 4: Experimental Parameters Associated with the Diffusion Process of α-Chymotrypsin As a Function of Size and Concentration of Crowding Agents Assuming a Uniform Circular Disc Profile Model

crowder	C (mg/mL)	τ_D (s)	α	D^{eff} (μm^2/s)
D1	100	0.7 ± 0.1	1.0 ± 0.1	80.4 ± 8.3
	200	2.7 ± 0.2	0.9 ± 0.1	20.6 ± 1.2
	300	6.2 ± 0.4	0.9 ± 0.1	9.0 ± 0.6
D2	50	7.0 ± 0.3	0.9 ± 0.1	7.9 ± 0.4
	100	8.2 ± 0.4	0.9 ± 0.1	6.7 ± 0.3
	200	11.3 ± 0.4	0.9 ± 0.1	4.9 ± 0.2
	300	16.0 ± 0.3	0.9 ± 0.1	3.5 ± 0.1
D3	50	9.5 ± 0.4	0.9 ± 0.1	5.9 ± 0.2
	100	10.4 ± 0.3	0.8 ± 0.1	5.3 ± 0.1
	200	13.5 ± 0.2	0.8 ± 0.1	4.1 ± 0.1
	300	32.0 ± 0.4	1.1 ± 0.1	1.7 ± 0.1

In samples with Dextrans as crowding agent, two types of diffusion behavior were obtained depending on concentration and size of obstacles. Tables 3 and 4 show the experimental parameters associated with the diffusion process of FITC-α-chymotrypsin as a function of size and concentration of Dextran assuming Gaussian intensity profile (eq 9) or uniform circular disk profile (eq 12) as analysis model, respectively.

First, in Tables 3 and 4 it can be seen that in samples with Dextran having a size smaller than FITC-α-chymotrypsin (Dextran with M_w = 5200 Da, called D1) the diffusional behavior of the protein depends on obstacle concentration. When the concentration of D1 is low (100 mg/mL) the resultant diffusion is practically normal ($\alpha \sim 1$) despite that the diffusion

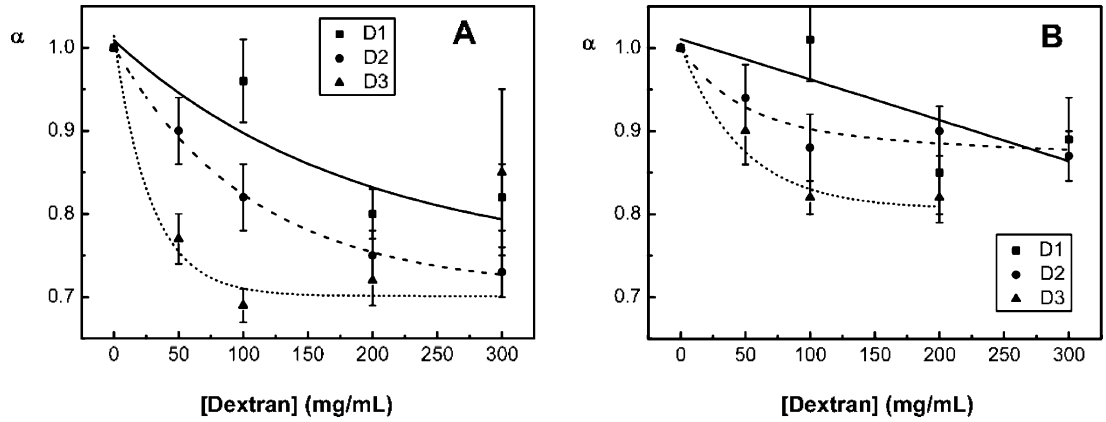

Figure 2. Anomalous diffusion exponent associated with the diffusion of α-chymotrypsin as a function of obstacle concentration for Dextrans of various average molecular weights (■) for D1, (●) for D2, and (▲) for D3. The plots obtained using the Gaussian profile model (A) and the uniform circular disk profile model (B) are shown.

is slower than in dilute solution. However, when increasing the D1 concentration, experimental fits show an anomalous diffusion behavior. In fact, a subdiffusional behavior is found ($\alpha < 1$). α decreases and τ_D increases as D1 concentration increases. Comparing the values for τ_D and α obtained in the presence of D1 from the best fit of the two analysis models, we see that the ones obtained assuming a Gaussian profile are slightly lower than those assuming uniform circular disk profile. However, as these differences fall within fitting errors, we can interpret that both methods give similar results.

Second, in Tables 3 and 4 it can also be seen the diffusional behavior of the protein in samples with Dextran having a size greater than FITC-α-chymotrypsin (Dextran with $M_w = 48\,600$ Da, called D2 and Dextran with $M_w = 409\,800$ Da, called D3). An increase of the diffusional time τ_D and a consistent decrease of the anomalous coefficient α for the protein is observed when the concentration of both Dextrans in solution is increased. Moreover, we can see a size-dependent emergence of anomalous subdiffusion that also clearly depends on the fractional volume occupied by the crowding agent. These experiments also confirm that the interaction via excluded volume could cause subdiffusion. Like in samples with 88% glycerol−water mixture and with different concentrations of D1, in both tables we see that in presence of different concentrations of D2 or D3 the τ_D values obtained by the best fits with both models are quite similar in all the studied samples within fitting errors. Although there are some small differences in the α-fitted values, the qualitative behavior of this parameter is similar for both models (Figure 2). In view of our results we can conclude that both fitting models can be used to characterize the diffusional behavior of α-chymotrypsin in concentrated Dextran solutions. In other words, despite having employed a confocal laser scanning microscope, in our experimental conditions we can use indistinctly the equations described by Axelrod et al.[42] and Soumpasis[47] for nonscanning microscopes with Gaussian and uniform circular disk laser beam, respectively.

From the parameters obtained in FRAP experiments and using eq 5, it is possible to calculate an effective diffusion coefficient, D^{eff}, for FITC-α-chymotrypsin in Dextran solutions. These values are also shown in Tables 3 and 4. D^{eff} for α-chymotrypsin in dilute solution has an approximate value of 114 $\mu m^2 s^{-1}$ (calculated using Stokes−Einstein equation). In these tables we can see that D^{eff} has a similar behavior as the anomalous diffusion parameter α, this means that D^{eff} decrease with increasing concentration and size (M_w) of obstacles.

Furthermore, Tables 3 and 4 show that when there is a concentration of 300 mg/mL of D3 in the samples, the value of τ_D obtained with both models is higher than it could be expected and α is equal to 1, which implies normal diffusion. This result indicates that there is a range of concentrations and/or sizes of crowding agents out of which the fitting expressions used here are not valid. One possible explanation is that in this case the protein could undergo a dimerization process causing that two different diffusion species are found in solution. It is known that α-chymotrypsin has a dimerization process at low pH.[61−64] In principle, in our experimental conditions, this protein should remain as a monomer. However, as crowding conditions could induce aggregation of proteins,[65] we carried out time-resolved fluorescence depolarization experiments with the purpose of verifying whether, in this case, there is homoaggregation. We examined the time-resolved anisotropy of FITC-α-chymotrypsin in dilute solution and in presence of different concentrations of the three Dextrans (data not shown). In all cases, two rotational correlation times were needed to describe the decay process ($1.7 \pm 0.2\ \mu s$ and $4.0 \pm 1.0\ \mu s$). As both rotational correlation times were similar in all the experiments we can conclude that there is not any kind of aggregation process in any case, including the sample with 300 mg/mL of D3. Despite this evidence, we tried to study the FRAP curves assuming that there were two species in the samples, monomer and dimer, with two different populations. However, the obtained results (data not shown) indicate that there was only one diffusional species in the 300 mg/mL D3 samples and no binding reaction. In addition, if there were a homodimer in this sample the value of D^{eff} obtained using Stokes−Einstein equation should be around 57 $\mu m^2\ s^{-1}$. But the obtained value, near to zero, indicates that the protein is practically still due to the high concentration of obstacles. This means that in this sample there is hardly free volume for the diffusion of the protein, a great part of the volume of the sample is occupied by obstacles. Another possibility is to consider a reaction-diffusion process in order to check whether a binding reaction with Dextrans or other proteins occurs. Thus, we studied our FRAP curves following the full reaction-diffusion scheme proposed by Sprague et al.[46] that uses a Laplace transform to obtain the FRAP response in the Laplace domain (eq 6 in ref 46). Although we obtained a good fitting, the results have not physical sense (results not shown) and cannot be taken into account. Thus, the additional tests that we have performed indicate that other phenomena such as hydrodynamic interactions,[7] microviscosity[7,65] or interplay between branches of Dextran polymers[66] must be considered in the fitting models to explain the diffusional results obtained in samples with a high concentration of obstacles with large sizes.

Finally, it is interesting to analyze the dependence of anomalous exponent α on the concentration and size of the Dextrans used as obstacles. In Figure 2a (for the Gaussian profile model) and Figure 2b (for the uniform circular disk profile model), we can see that α decays with increasing obstacle concentration and this decay becomes steeper with increasing the obstacle size (average molecular weight of Dextran). As the time scale of confocal FRAP experiments is very short, we could observe the time-dependence of the diffusion coefficient of α-chymotrypsin in crowded Dextran solutions but it was not possible to obtain its limiting value corresponding to the long time normal diffusion, D^*. The effective diffusion coefficient values, D^{eff}, reported in Tables 3 and 4, are characteristic parameters that describe the diffusion at the scale of the beam area.

Although there is an important number of works that study anomalous diffusion of macromolecules in crowded media using Monte Carlo simulations,[9–11] the number of experimental studies devoted to this phenomenon is considerably smaller. Some of them show clear evidence of anomalous subdiffusion, mainly in 2D media, for example, in lipid bilayers[25,35] or in cell surfaces.[25,34] However, there are few experimental works showing anomalous subdiffusion in 3D media, mainly in crowded solution.[23,29,30] Our results are in qualitative agreement with these previous studies. In fact, the dependence of the anomalous diffusion behavior of the α-chymotrypsin on the size and concentration of Dextrans that we have observed in our experiments is in agreement with the conclusions of Banks and Fradin[23] in their study of the diffusion of streptavidin in highly concentrated solutions of bovine serum albumin (BSA), streptadivin, and Dextrans with different molecular weights. Thus, the size and the concentration of the obstacles play a very important role in the diffusion processes in macromolecular crowded media and should be taken into account in future studies about reaction diffusion in crowded media.

Conclusions

In this work, we have checked that FRAP curves obtained under our experimental conditions with confocal laser scanning microscope can be studied using either the Gaussian or the uniform circular disk profile model for nonscanning microscopes. The generalized equations to take into account anomalous diffusion provided by these two models yield a similar diffusional behavior of α-chymotrypsin in solution crowded media of Dextran, indicating that anomalous diffusion takes place. The concentration and size of the crowding agent are two important factors that determine the existence and degree of the anomalous diffusion of α-chymotrypsin in crowded media, until a high concentration of large size Dextran is reached. Beyond this limit other phenomena such as microviscosity, hydrodynamics interaction or interplay between branches of Dextran polymers should probably be considered.

Acknowledgment. We thank to Professor H. Qian for his interesting commentaries about our work, which have contributed in a great extent to the compression of our problems. We thank to the three anonymous referees for their comments about our manuscript, which have been very important in the better explanation of our work. This work was supported by the Spanish Ministry of Science and Technology (Projects CTM2006-13583 and SAF2008-00164), by Red Temática de Investigación Cooperativa en Cáncer, Instituto de Salud Carlos III (ISCII-RTICC (RD06/0020/0046 and RD06/0020/1037)) and by the Generalitat de Catalunya (Grants 2009SGR465 and 2009SGR1308 and XRQTC). I.P. thanks to Juan de la Cierva Program of Spanish Ministry of Science.

References and Notes

(1) Minton, A. P. *J. Biol. Chem.* **2001**, *276*, 10577.
(2) Ellis, R. J. *Trends. Biochem. Sci.* **2001**, *26*, 597.
(3) Ellis, R. J.; Minton, A. P. *Nature* **2003**, *425*, 27.
(4) Derham, B. K.; Harding, J. J. *Biochim. Biophys. Acta* **2006**, *1764*, 1000.
(5) Zhou, H. X.; Rivas, G.; Minton, A. P. *Annu. Rev. Biophys.* **2008**, *37*, 375.
(6) Agrawal, M.; Santra, S. B.; Anand, R.; Swaminathan, R. *PRAMANA J. Phys.* **2008**, *71*, 359.
(7) Dix, J. A.; Verkman, A. S. *Annu. Rev. Biophys.* **2008**, *37*, 247.
(8) Zhou, H. X. *J. Phys. Chem. B.* **2009**, *113*, 7995.
(9) Saxton, M. J. *Biophys. J.* **1994**, *66*, 394.
(10) Saxton, M. J. *Biophys. J.* **2001**, *81*, 2226.
(11) Isvoran, A.; Vilaseca, E.; Garcés, J. L.; Unipan, L.; Mas, F. Proceedings of the 6th Conference of Balkan Physics Union, A. I. P., Istanbul, August 22–27, 2006; 2007; Vol. 889, p 469.
(12) Saxton, M. J. *Biophys. J.* **1987**, *52*, 989.
(13) Saxton, M. J. *Biophys. J.* **1990**, *58*, 1303.
(14) Saxton, M. J. *Biophys. J.* **1993**, *64*, 1053.
(15) Isvoran, A.; Vilaseca, E.; Unipan, L.; Garcés, J. L.; Mas, F. *Rom. Biophys. J.* **2007**, *17*, 21.
(16) Isvoran, A.; Vilaseca, E.; Unipan, L.; Garcés, J. L.; Mas, F. *Rev. Rom. Chem.* **2008**, *53*, 415.
(17) Dix, J. A.; Han, E. F. Y.; Verkman, A. S. *J. Phys. Chem. B* **2006**, *110*, 1896.
(18) Kao, H. P.; Abney, J. R.; Verkman, A. S. *J. Cell Biol.* **1993**, *120*, 175.
(19) Olveczki, B. P.; Verkman, A. S. *Biophys. J.* **1998**, *74*, 2722.
(20) Wachsmuth, M.; Waldeck, W.; Langowski, J. *J. Mol. Biol.* **2000**, *298*, 677.
(21) Arrio-Dupont, M.; Foucault, G.; Vacher, M.; Devaux, P. F.; Cribier, S. *Biophys. J.* **2001**, *78*, 901.
(22) Fradin, C.; Abu-Arish, A.; Granek, R.; Elbaum, M. *Biophys. J.* **2003**, *84*, 2005.
(23) Banks, D. S.; Fradin, C. *Biophys. J.* **2005**, *89*, 2960.
(24) Franks, F. *Protein biotechnology. Isolation, characterization and stabilization*; Franks, F., Ed.; Humana Press: Clifton, NJ, 1993; p 133.
(25) Schwille, P.; Korlach, J.; Webb, W. W. *Cytrometry* **1999**, *36*, 176.
(26) Fatin-Rouge, N.; Milon, A.; Buffle, J.; Goulet, R. R.; Tessier, A. *J. Phys. Chem. B* **2003**, *107*, 12126.
(27) Weiss, M.; Elsner, M.; Kartberg, F.; Nilsson, T. *Biophys. J.* **2004**, *87*, 3518.
(28) Szymański, J.; Patkowki, A.; Gapiński, J.; Wilk, A.; Holyst, R. *J. Phys. Chem. B* **2006**, *110*, 7367.
(29) Sanabria, H.; Kinbota, Y.; Waxham, M. N. *Biophys. J.* **2007**, *92*, 313.
(30) Reitan, N. K.; Juthajan, A.; Lindmo, T.; de Lange Davias, C. *J. Biomol. Opt.* **2008**, *13*, 054040.
(31) Cherdhirakorn, T.; Best, A.; Koynov, A.; Peneva, K.; Muellen, K.; Fytas, G. *J. Phys. Chem. B* **2009**, *113*, 3355.
(32) Feder, T. J.; Brust-Mascher, I.; Slattery, J. P.; Baird, B.; Webb, W. W. *Biophys. J.* **1996**, *70*, 2767.
(33) Periasamy, N.; Verkman, A. S. *Biophys. J.* **1998**, *75*, 557.
(34) Pyenta, P. S.; Schwille, P.; Webb, W. W.; Holowka, D.; Baird, B. *J. Phys. Chem. A* **2003**, *107*, 8310.
(35) Ratto, T. V.; Longo, M. L. *Langmuir* **2003**, *19*, 1788.
(36) Dunham, S. M.; Pudavar, H. E.; Prasad, P. N.; Stachowiak, M. K. *J. Phys. Chem. B* **2004**, *108*, 10540.
(37) Heitzman, C. E.; Tu, H.; Braun, P. V. *J. Phys. Chem. B* **2004**, *108*, 13764.
(38) Pucadyil, T. J.; Chattopadhyay, A. *J. Fluorescence* **2006**, *16*, 87.
(39) Pujalyil, T. J.; Mukherjee, S.; Chattopadhyay, A. *J. Phys. Chem. B* **2007**, *111*, 1975.
(40) Lukelski, A.; Klafter, J. *Biophys. J.* **2009**, *96*, 2055.
(41) Braga, J.; Desterro, J. M. P.; Carmo-Fonseca, M. *Mol. Biol. Cell* **2004**, *15*, 4749.
(42) Axelrod, D.; Koppel, D. E.; Schlessinger, J.; Elson, E.; Webb, W. W. *Biophys. J.* **1976**, *16*, 1055.
(43) Blonk, J. C. G.; Don, A.; Aalst, H. V.; Birmingham, J. J. *J. Microsc.* **1992**, *169*, 363.
(44) Kubitscheck, U.; Wedekind, P.; Peters, R. *Biophys. J.* **1994**, *67*, 948.
(45) Braeckmans, K.; Peeters, L.; Sanders, N. N.; De Smedt, S. C.; Demeester, J. *Biophys. J.* **2003**, *85*, 2240.
(46) Sprague, B. L.; Pego, R. L.; Stavreva, D. A.; McNally, J. G. *Biophys. J.* **2004**, *86*, 3473.
(47) Soumpasis, D. M. *Biophys. J.* **1983**, *41*, 95.

(48) Kang, M.; Day, A. C.; Drake, K.; Kenworthy, A. K.; DiBenedetto, E. *Biophys. J.* **2009**, *97*, 1501.
(49) Fundueanu, G.; Nastruzzi, C.; Carpov, A.; Desbrieres, J.; Rinaudo, M. *Biomaterials* **1999**, *20*, 1427.
(50) Schaefer, D. W.; Martin, J. E.; Wiltzius, P.; Cannell, D. S. *Phys. Rev. Lett.* **1984**, *52*, 2371.
(51) Diehl, H.; Horchak-Morris, N. *Talanta* **1987**, *34*, 739.
(52) Bouchaud, J. P.; Georges, A. *Phys. Rep.* **1990**, *185*, 127.
(53) Metzler, R.; Klafter, J. *Phys. Rep.* **2000**, *339*, 1.
(54) Havlin, S.; Ben-Avraham, D. *Adv. Phys.* **1987**, *36*, 695.
(55) Almedia, P.; Vaz, W. Lateral diffusion in membranes. In *Handbook of Biological Physics*; Lipowsky, R., Sackmann, E., Eds.; Elsevier: New York, 1995; p 305.
(56) Saxton, M. J. *Biophys. J.* **2007**, *92*, 1178.
(57) Saxton, M. J. *Biophys. J.* **1996**, *70*, 1250.
(58) Yguerabide, J.; Schimidt, J. A.; Yguerabide, E. E. *Biophys. J.* **1982**, *39*, 69.
(59) Elson, E. L. *Annu. Rev. Phys. Chem.* **1985**, *36*, 379.
(60) Lide, D. R. *CRC Handbook of chemistry and physics*, 89th ed.; CRC Press: Boca Raton, FL, 2008.
(61) Rao, M. S. N.; Kegeles, G. *J. Am. Chem. Soc.* **1658**, *80*, 5724.
(62) Winzor, D. J.; Scheraga, H. A. *J. Phys. Chem.* **1964**, *68*, 338.
(63) Aune, K. C.; Goldsmith, L. C.; Timasheff, S. N. *Biochemistry* **1971**, *10*, 1617.
(64) Patel, C. N.; Noble, S. M.; Weatherly, G. T.; Tripathy, A.; Winzor, D. J.; Pielak, G. J. *Protein Sci.* **2002**, *11*, 997.
(65) Verkman, A. S. *Trends Biochem. Sci.* **2002**, *27*, 27.
(66) Ioan, C. E.; Aberle, T.; Burchard, W. *Macromolecules* **2000**, *33*, 5730.

JP910811J